Dependence of deposition parameters and layer thickness on the characteristics of Nd-Fe-B thin films

Dependence of deposition parameters and layer thickness on the characteristics of Nd-Fe-B thin films

S Madeswaran[1], R Tokumaru[2], S Tamano[2], S Goto[2], K Tokiwa[1,2] and T Watanabe[1]

[1]Polyscale Technology Research Center, Tokyo University of Science
2641 Yamazaki, Noda, Chiba 278-8510, Japan

[2]Department of Applied Electronics, Tokyo University of Science, Japan
2641 Yamazaki, Noda, Chiba, 278-8510, Japan

E-mail: smades@rs.noda.tus.ac.jp

Abstract. Textured Nd-Fe-B thin films with hard magnetic properties were prepared on a Ta (110) buffer layered glass substrates using radio frequency (RF) sputtering deposition. We investigated the influence of substrate temperature, sputtering gas pressure, RF power and film thickness on their microstructural and magnetic properties. Composition in the Nd-Fe-B thin films prepared using the same target with an Nd/Fe ratio of 0.32 was markedly changed (varied between 0.21 and 0.31) depending on the Ar pressure and the RF power. Well-textured Nd-Fe-B films grown at a deposition pressure of 7.0 Pa, a temperature of 550 ˚C, and a power of 100 W revealed better magnetic properties: J_r=1.1 T, H_c = 1130 kA/m and $BH_{(max)}$ = 236 kJ/m^3.

1. Introduction

Recent investigations on the hard magnetic Nd-Fe-B thin films with easy magnetization axis have opened up great possibilities of applications like micro-electro-mechanical devices [1] and data recording media [2]. The Nd-Fe-B magnets have also extended for high power actuators and susceptible to high temperature irreversible demagnetization [3] owing to their high energy product value. The high energy product value depends on high remanence and high coercivity that always enhances the performance of a device [4]. The remanence values are greatly influenced by the grains alignment which is considerably attained by the texturing of the sample [5, 6]. The coercivity has at least half the value of remanence for a high performance film. The intrinsic properties of the magnetic phase and the direct exchange or long-range magnetostatic interactions between the grains of phases are the deciding factors of coercivity of the magnetic materials. Microstructure of a magnetic material plays a key role in determining the interaction mechanism. Therefore, the study on microstructure is not only essential for understating the magnetic phenomena but for tailoring the magnetic properties.

In general, the strong c-axis orientation and enhanced perpendicular magnetic properties in the crystallized films are potentially modified by the deposition process [7]. Several works were reported on the effects of deposition parameters on Nd-Fe-B films properties [8-10]. However, in these reports, the film properties seemingly varied very much depending on the deposition methods used for film preparation apart from the deposition parameters. The suitable conditions for making aligned films are more likely depending on the sputtering system besides the substrate material, target composition,

substrate temperature, sputtering gas atmosphere, and deposition rate [6, 8-11]. In this report the effects of various process parameters on the magnetic properties of Nd-Fe-B films prepared by RF sputtering are investigated.

2. Experiment

The films were deposited in a high vacuum chamber with a base pressure of ~10^{-5} Pa by sputtering a Nd-rich target with a nominal composition of $Nd_{20}Fe_{64}B_{16}$ prepared by Spark Plasma Sintering. Ta buffer layer with the thickness of 50 nm was deposited onto the glass substrate prior to depositing the Nd-Fe-B film, to enable texturing of $Nd_2Fe_{14}B$ phase and also to prevent diffusion of the substrate materials into the film [12]. A cap layer of 20 nm thick Ta was also deposited over the Nd-Fe-B film to product it from oxidation on contact with air. A resistive heater was used to regulate the substrate heating. The films were grown at substrate temperatures (T_s) of 300, 400 and 500 ˚C and the sputter power varied between 50 and 150 W. The distance between target and substrate was fixed at 60 mm. The sputtering Ar gas pressure was changed from 1 to 17 Pa. A sputter rate of 20 nm /min at 100 W was used to study the effect of film thickness. While we adjusted one deposition parameter, all others were remaining unchanged. X-ray analysis was performed with a Rigaku Ultima-III diffractometer utilizing Cu-Ka radiation. Microstructural investigations were performed with a Hitachi S-4200 digital scanning electron microscope (SEM), equipped with energy dispersive X-ray (EDX) detector. The film thickness was measured by cross-sectional SEM. Magnetic properties were measured by Vibrating Sample Magnetometer (VSM) with a maximum field of 20 kOe. The magnetic properties were measured both perpendicular and parallel direction to the film plane.

3. Results and Discussion

3.1. Effect of Temperature

The XRD patterns of as-deposited films [layer form-Ta(50nm)/NdFeB(300nm)/Ta(20nm)] grown at temperature between 300 and 500 ˚C on a Ta-buffered glass substrate at a power of 100W and a Ar pressure of 7 Pa are shown in figure 1. For the film deposited at temperature 300 ˚C, peaks of $Nd_2Fe_{14}B$ crystalline phase are absent, however, Ta (110) and a peak at 2θ= 33.5˚ that may corresponding Fe_3B phase (JCPDS data 34-1198) appear, indicating that the Nd-Fe-B film is amorphous. When T_s increases from 300 to 400 ˚C, another peak emerges at 44.6˚ which can be attributed to (006) of $Nd_2Fe_{14}B$ or α-Fe phase. In the case of film deposited at 500 ˚C, high intensity peaks corresponding (004), (006) and (008) plane of crystalline $Nd_2Fe_{14}B$ phase occur with a strong (00*l)* texture, tending to be perpendicular to the plane of the film. Additionally, the x-ray pattern also shows that there are some inclusions of Nd-rich and Nd_xO_y phases. Based on the reports by Minowa et al (13) and Yue et al (14), it can be say that the Nd-rich phase consists of complex Nd containing intermetallic compound and Nd_xO_y. Note that regardless of different deposition temperatures, all these films show the presence of Fe_3B phase.

Figure 2 shows the XRD patterns for the films deposited at 300, 400, and 500 ˚C after being annealed at 600 ˚C for 15 min. Of the three films, the film deposited at 500 ˚C exhibited notably high intensity peaks of the (004), (006) and (008) plane which are the most intense in the tetragonal $Nd_2Fe_{14}B$ phase with the preferred *c*-axis orientation perpendicular to the plane of the film. This suggests that annealing treatment eventually enhances the crystallization in the film grown at a higher deposition temperature than the films grown relatively at lower temperatures. This is more evident in case of the 004 peak with increased sharpness. It is interesting to note that the peak appeared at 33.5˚ in the as-deposited state completely disappeared after annealing, suggesting that it might be related to the unstable Fe_3B phase in these films.

The magnetic behavior measured by VSM (figures not shown) showed soft magnetic phases for as- deposited films at 300 and 400˚C whereas the film deposited at 500 ˚C revealed hard magnetic phase. This is consistent with x-ray diffraction data displayed in figure 1. The hysteresis loops measured at room temperature for the films annealed at 600 ˚C are shown in figure 3. The solid and dashed lines represent measuring field direction along perpendicular (out-plane-⊥) and parallel (in-

plane-||) to the film plane, respectively. No demagnetization correction was performed for any of the measurement. The loops indicate that the film grown at 500 ˚C and annealed at 600 ˚C demonstrated better magnetic properties when compared to the ones grown at lower temperatures after annealing at the same temperature. It can also be seen that the ratio of $J_{r\perp}$ / $J_{r\parallel}$ for the film deposited at 500 ˚C is higher (3.2) than the films deposited at 300 and 400˚C (2.2 and 2.5 respectively). Being consistent with the XRD results, the magnetic properties also confirm that better crystallization of magnetic $Nd_2Fe_{14}B$ phase occurs only for direct deposition at high temperature while it is less for the films produced at low temperatures and annealed at high temperature. Tang *et al* [7] observed constant out-plane coercivity, H_c, for both low and high temperature deposition with subsequent annealing at high temperature. This is mainly because of different target composition, i.e, high Nd content in our case, which leads to the parallel growth of Nd-rich and Nd_xO_y phases. It is expected that the Nd_xO_y phase might support the growth of $Nd_2Fe_{14}B$ phase with c-axis texture when the deposition temperature is high, however, it hinders growth of the texturing $Nd_2Fe_{14}B$ phase at low deposition temperatures and subsequent annealing treatment [11, 15].

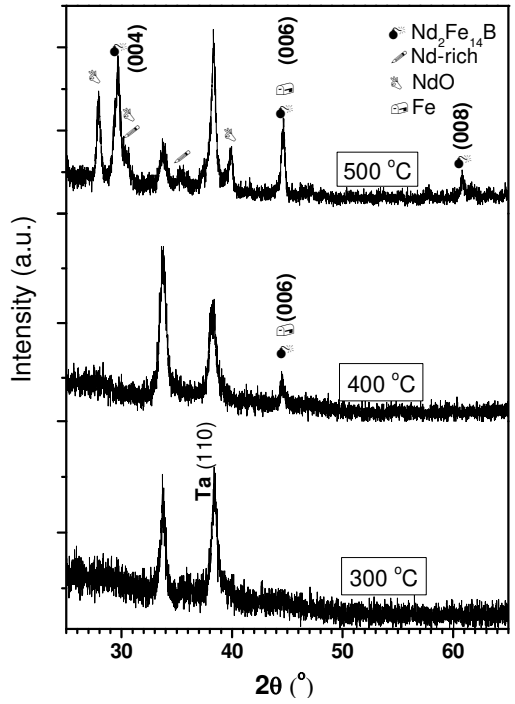

Figure 1. XRD patterns for the films deposited at different substrate temperature.

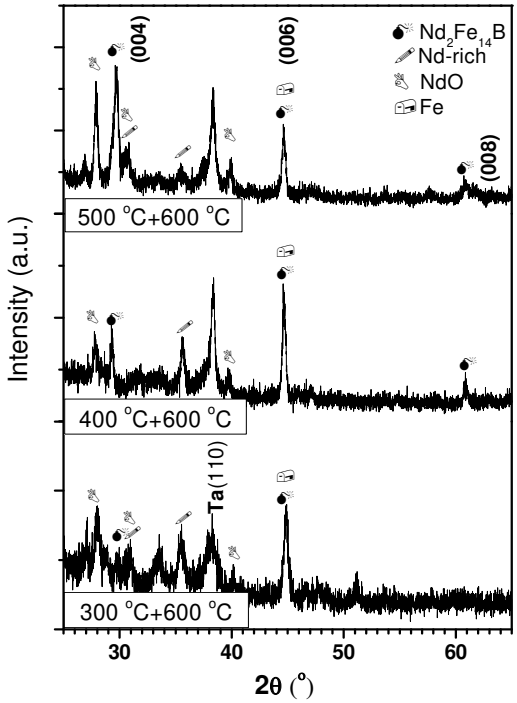

Figure 2. XRD patterns for the films deposited at different substrate temperature and annealed at 600 ˚C.

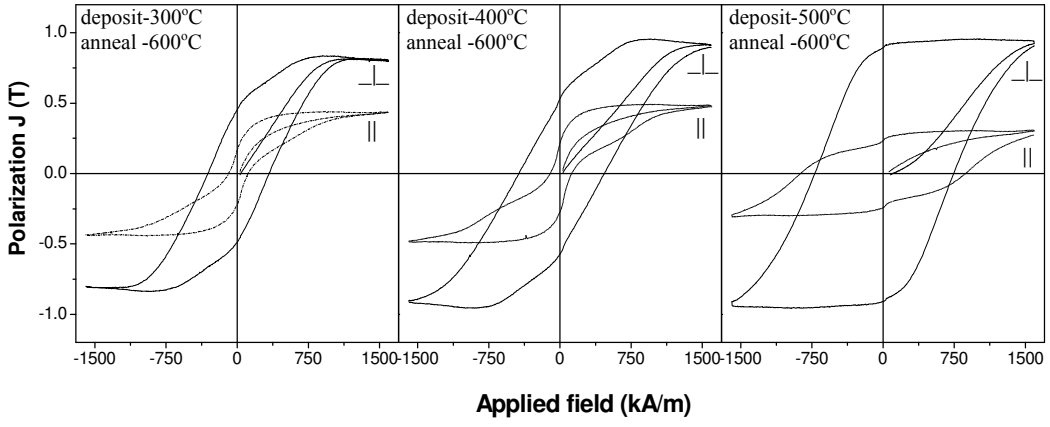

Figure 3. Hysteresis loops of films deposited at different substrate temperature and annealed at 600 ˚C.

3.2. Effect of Ar gas Pressure

We observed considerable variation in the microstructure and magnetic properties of the Nd-Fe-B films while varying Ar gas pressure from 1 to 17 Pa under fixed sputter power and deposition temperature (100 W and 550 ˚C, respectively). XRD patterns of the films deposited under 1, 10 and 17 Pa are shown in figure 4. For all the films, c-axis texturing could be obtained; however the intensities and sharpness of the peaks are weak for low Ar pressure and phases of Nd-rich and Nd_xO_y get strengthened at high Ar pressure. Surface morphologies of these films, observed by SEM (images are not shown), indicated the grain size increases with increasing Ar pressure due to the fact that composition in the films vary accordingly. EDX analysis of the films deposited at different Ar pressures with same target composition indicates remarkable changes in the film composition (see Table 1). Table 1 shows the increase of ratio between Nd and Fe (Nd/Fe=0.21-0.31) for increasing Ar pressure. Liu *et al* [8] and Parhofer *et al* [16] showed the same trend while increases the ambient pressure. The Ar pressure during sputter greatly influences the kinetic energy of the elements on the substrate surface and hence change of composition and grain size of the films. If the gas pressure is very high, it may also lower the kinetic energy of the species in the plasma due to their intensive collisions with gas atoms, which resulted in the further drop of Nd/Fe (0.26) value for 17 Pa.

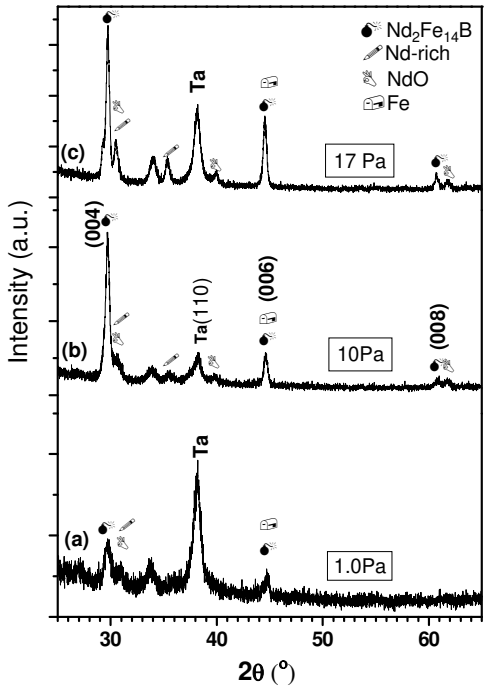

Figure 4. XRD patterns of the Nd-Fe-B films prepared under various Ar pressure.

Table 1. Ratios of Nd and Fe in the film deposited under various pressures are listed.

Ar (Pa)	Nd/Fe	Ar (Pa)	Nd/Fe
1.0	0.21	10.0	0.28
2.5	0.24	12.5	0.31
5.0	0.25	17.0	0.26
7.5	0.26		

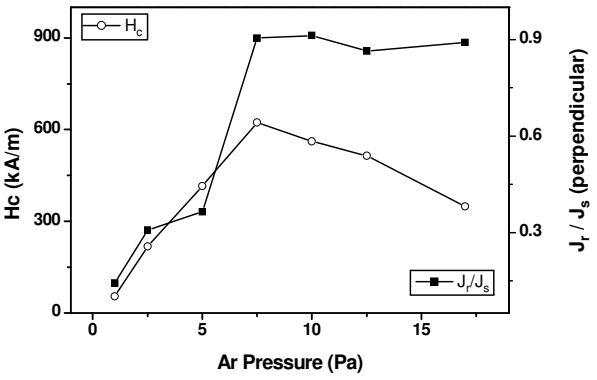

Figure 5. Ar pressure dependence on the coercivity and reduce romance of film measured along perpendicular to the film plane.

The effect of ambient gas pressure on magnetic properties of the Nd-Fe-B films is illustrated in figure 5. The reduced remanence i.e., ratio of remanence and saturation magnetization (J_r/J_s) is very low for the film prepared at very low Ar pressure. For the pressure up to 7 Pa, the reduced remanence increases and reaches close to unity and then remains almost constant for further increase of Ar pressure. It seems that the texturing of the films is better for the conditions of Ar pressure from 7 to 17 Pa. This is consistent with the result demonstrated by the x-ray diffraction data in figure 4. It is of note that Liu et al [8] observed decrease of remanence polarization with increasing Ar pressure that is

different for our case. We presume that the properties of the films under study largely depend on the processing parameters such as target composition, sputter rate, etc. The increase in coercivity of the films grown at Ar pressures between 1 and 7 Pa is due to the Nd-rich phase formation. Further decrease of coercivity for increasing pressure beyond 7 Pa may perhaps be due to: (1) better alignment of the $Nd_2Fe_{14}B$ grains which makes easier magnetization reversal of whole layer once a reversed domain is formed, (2) larger grain size for which the domain wall movement occur considerably at low applied field, and (3) formation of the oxidized Nd phase.

3.3. Effect of sputter power

The effect of RF power on magnetic properties of Nd-Fe-B films was studied since the deposition rate is effectively changing according to sputter power that plays an important role in determining the magnetic behavior [9, 17, 18]. Nd-Fe-B films of about 500 nm thickness were deposited at different sputter power (50, 75, 100 and 150 W) while the substrate temperature and Ar pressure were fixed, respectively, at 550 ˚C and 7 Pa. The deposition rates of the films varied between 14 and 22 nm/min for different RF powers used. The surface morphology of films grown at various RF powers is depicted in figure 6. It can be clearly noticed that drastic variation in grain size as well as in shape for each RF power. Closely packed spherical shapes with average grain size of about 150 nm and island like spherical shape with average grain size of ~400 nm were observed for 50 and 75 W, respectively. For 100 W, platelet shape of 500 nm size was revealed. Rectangular shape with different size in different orientation could be obtained for the film prepared at 150 W. The increase of deposition rate will raise the Nd/Fe ratio which was already proved by Chen et al [18]. The rising values of Nd/Fe ratio were verified by EDX and they are 0.21, 0.24, 0.26 and 0.29 for 50, 75, 100 and 150 W, respectively. Nd_xO_y reflections observed by XRD are higher for the film deposited at 150 W and hence we expect that the presence of bimodal gains in it. The difference in gains is not only due to the variation in Nd content but also due to the difference in crystalline growth by bombardment of different energy particles emitted from the target [9].

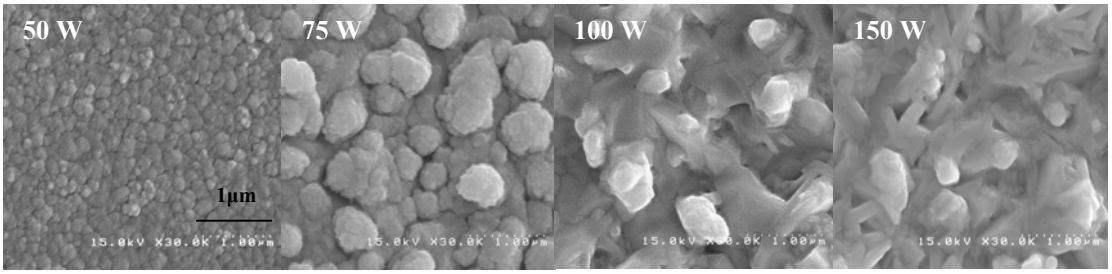

Figure 6. SEM images of films deposited at various sputter power.

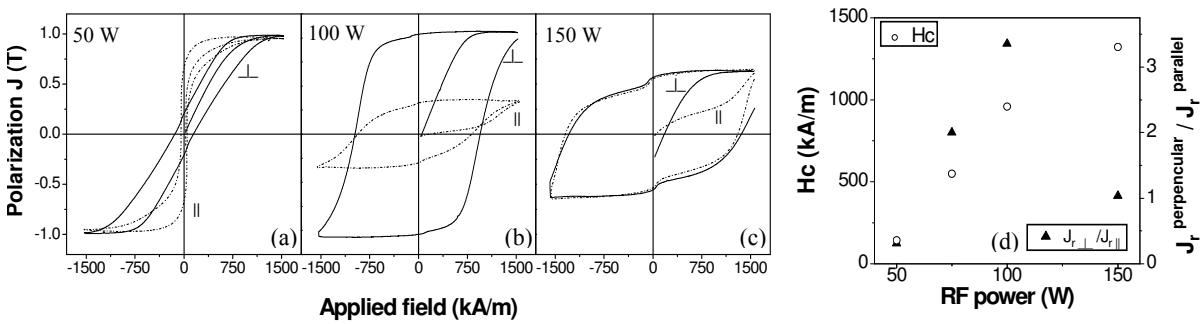

Figure 7. Hysteresis loops of the films deposited at different sputter power (a, b and c) and dependence of magnetic properties on power (d).

Figures 7 a-c show the typical hysteresis loops measured for the films grown at various power. Film sputtered at low power exhibits less hard magnetic behavior as it has less Nd content and poor anisotropic. For the power 100 W, the remanence polarization, $J_{r\perp}$, is much higher than $J_{r\parallel}$. It implies the existence of texture along c-axis which is perpendicular to film's plane. But for 150 W, the $J_{r\perp}$ and $J_{r\parallel}$ are almost same since the perpendicular anisotropic is deteriorated. The low saturation magnetization is due to the formation of non-magnetic phase as observed by XRD. Sputter power dependence on coercivity, H_c, and ratio between $J_{r\perp}$ and $J_{r\parallel}$ are shown in figure 7d. The coercivity is rising almost linearly with increasing the RF power; this is because of coexistence of the hard magnetic $Nd_2Fe_{14}B$ phase together with Nd-rich intergranular phase in the film. It is quite obvious that coercivity is sensitive to the composition of the film and high Nd concentration in the film results to the high coercivity [18]. Increase in the ratio of $J_{r\perp}$ and $J_{r\parallel}$ up to 100 W shows the increase of perpendicular anisotropic behavior and it decreases for further increase of power indicates the isotropic phase formation.

3.4. Effect of film thickness

Figure 8 plots coercivity, H_c, and reduced remanence (in perpendicular direction), J_r/J_s, with respect to various film thicknesses of samples grown at 550 ˚C, 7.0 Pa and 100 W. The trend of J_r/J_s shows that the texturing is better from 50 nm and above. The maximum coercivity (~1130 kA/m) was observed for a 100 nm thin film. It has been reported that the coercivity is not only influenced by the texture, but on grain size as well [5]. There may be an optimum grain size of $Nd_2Fe_{14}B$ with high coercivity for the film prepared by RF sputtering. For very thin film, the higher possibility of relative volume percentage of oxidized or defect layer hinters the nucleation field of the hard magnetic phase [10]. The H_c decrease with increasing the thickness from 100 nm, which is due to the increased grain size that was observed by SEM (image is not shown here). If the grain size is very large, the exchange coupling between soft and hard magnetic phase is tough and the domain wall motion will be easy and thus the films will have comparatively low coercivity. Figure 10 shows typical hysteresis loops for the film of 100 nm thickness and measured in the direction of perpendicular and parallel to film plane. For this condition, the Nd-Fe-B film with the values of H_c = 1130 kA/m, J_r =1.2 T and $BH_{(max)}$ = 236 kJ/m^3 in perpendicular direction were obtained.

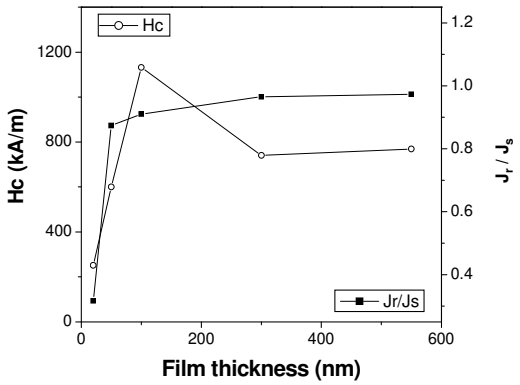

Figure 8. Influence of Nd-Fe-B film thickness on coercivity and reduced remanence.

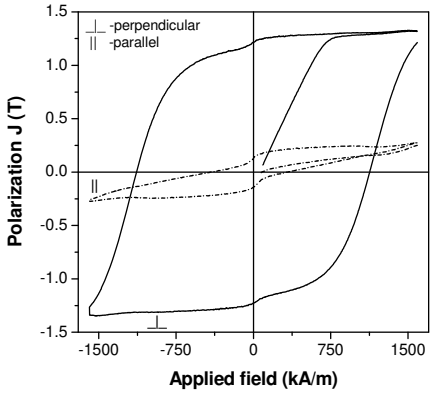

Figure 9. Hysteresis loops for a 100 nm thin Nd-Fe-B film grown at 550 ˚C, 7.0 Pa and 100 W.

4. Conclusion

We have prepared Nd-Fe-B thin films to study the correlations between deposition parameters of RF sputtering system and their microstructure and magnetic properties. The effect of deposition

temperature on the properties of films suggested that amorphous Nd-Fe-B films grew up to 400 ˚C, and film grown at 500 ˚C had better phase formation with good texture. The Nd/Fe ratio in the film was adjustable by varying the Ar pressure and RF power. Microstructure analysis revealed that the gain size and shape are greatly influenced by RF power. Magnetic results indicated that the Nd-rich films led to higher coercivity. Excellent magnetic properties with a romance of 1.1 T and a coercivity of 960 kA/m were achieved when the film grown at a moderate RF power of 100 W. Films exhibited deterioration in their anisotropic behavior for RF power >100 W. The maximum energy product as high as 236 kJ/m^3 was obtained for a 100 nm film deposited at 550 ˚C under 7.0 Pa, Ar pressure and with a RF power of 100 W.

Acknowledgement
This investigation was supported by "Academic Frontier" Project for Private Universities: matching fund subsidy from MEXT (Ministry of Education, Culture, Sports, Science and Technology), 2006-2010.

References:
[1] Chin T -S 2000 *J. Magn. Magn. Meter.* **209** 75
[2] Mapps D J, Chandrasekhar R, O'Grady K, Camdridge J, Petford A and Doole R 1997 *IEEE Trans. Magn.* **33** 3007
[3] Belmans R and Hameyer K 1998 *Proceedings of the Sixth International conference on New Actuators* (Bremen, Germany) p 537
[4] Gutfleisch O 2000 *J. Phys. D: Appl. Phys.* **33** R157
[5] Parhofer S, Kuhrt C, Wecker J, Gieres G and Schultz L 1998 *J. Appl. Phys.* **83** 2735
[6] Kwon A R, Fähler S, Neu V and Schultz L 2006 *J. Magn. Magn. Meter.* **302** 252
[7] Tang S L, Gibbs M R J , Davies H A, Mateen N E, Nie B and Du Y W 2008 *J. Appl. Phys.* **103** 07E113
[8] Liu W F, Suzuki S and Machida K 2007 *J. Magn. Magn. Mater.* **308** 126
[9] Piramanayagam S N, Matsumoto M and Morisako A 1999 *J. Appl. Phys.* **85** 5898
[10] Huang X J, Xu S Y, Ong C K, Yang Z, Si L and Li Y 2002 *J. Appl. Phys.***91** 4666
[11] Chen S L, Zheng J G, Liu W and Zhang Z D 2007 *J. Phys. D: Appl. Phys.* **40** 1816
[12] Hannemann U, Fähler S, Oswald S, Holzpfel B and Schultz L 2002 *J.Magn. Magn. Mater.* **242** 1294
[13] Minowa T, Shimao M, Honshima M 1991 J. Magn. Magn. Mater. **97** 107
[14] Yue M, Zhang J X, Liu W Q, Wang G P 2004 J. Magn. Magn. Mater. **271** 364
[15] Serrona L K E B, Sugimura A, Adachi N, Okuda T, Ohsato H, Sakamoto I, Nakanishi A, Motokawa M, Ping D H and Hono K 2003 *Appl. Phys. Lett.* **82** 1751
[16] Parhofer S, Gieres G, Wecker J and Schultz L 1996 *J. Magn. Magn. Mater*. **163** 32
[17] Cadieu F J, Cheung T D, Wickramasekara L and Kamprath N 1986 *IEEE Trans. Magn.* **22** 752
[18] Chen S L, Liu W and Zhang Z D 2006 *J. Magn. Magn. Mater.* **302** 306